The Fluoroquinolone Levofloxacin Triggers the Transcriptional Activation of Iron Transport Genes That Contribute to Cell Death in *Streptococcus pneumoniae*

María-José Ferrándiz,[a] **Adela G. de la Campa**[a,b]

Unidad de Genética Bacteriana, Centro Nacional de Microbiología, Instituto de Salud Carlos III and CIBER Enfermedades Respiratorias, Majadahonda, Madrid, Spain[a]; Presidencia, Consejo Superior de Investigaciones Científicas, Madrid, Spain[b]

We studied the transcriptomic response of *Streptococcus pneumoniae* to levofloxacin (LVX) under conditions inhibiting topoisomerase IV but not gyrase. Although a complex transcriptomic response was observed, the most outstanding result was the upregulation of the genes of the *fatDCEB* operon, involved in iron (Fe^{2+} and Fe^{3+}) uptake, which were the only genes varying under every condition tested. Although the inhibition of topoisomerase IV by levofloxacin did not have a detectable effect in the level of global supercoiling, increases in general supercoiling and *fatD* transcription were observed after topoisomerase I inhibition, while the opposite was observed after gyrase inhibition with novobiocin. Since *fatDCEB* is located in a topological chromosomal domain downregulated by DNA relaxation, we studied the transcription of a copy of the 422-bp (including the P_{fat} promoter) region located upstream of *fatDCEB* fused to the *cat* reporter inserted into the chromosome 106 kb away from its native position: $P_{fat}fatD$ was upregulated in the presence of LVX in its native location, whereas no change was observed in the $P_{fat}cat$ construction. Results suggest that topological changes are indeed involved in $P_{fat}fatDCE$ transcription. Upregulation of *fatDCEB* would lead to an increase of intracellular iron and, in turn, to the activation of the Fenton reaction and the increase of reactive oxygen species. In accordance, we observed an attenuation of levofloxacin lethality in iron-deficient media and in a strain lacking the gene coding for SpxB, the main source of hydrogen peroxide. In addition, we observed an increase of reactive oxygen species that contributed to levofloxacin lethality.

*S*treptococcus pneumoniae (the pneumococcus) acts as an opportunistic pathogen. It forms part of the commensal microbiota of the human nasopharynx. Under specific circumstances, it migrates to other niches (ear, lung, bloodstream, and cerebrospinal fluid) causing diverse pathologies. One million children aged <5 years die annually of pneumococcal infections worldwide (1). After the usage of the pneumococcal 7-valent conjugate vaccine, which includes the serotypes more often associated with resistance to antibiotics, the incidence of invasive pneumococcal disease declined (2, 3) coincidentally with a decrease of penicillin resistance rates in many countries (3–5). However, the emergence of serotypes not included in the vaccine has been observed (6, 7). Therefore, knowledge of the molecular bases of antimicrobial action, including the mechanisms of killing, is essential for developing improved therapeutics.

Resistance in *S. pneumoniae* to antibiotics acting either in cell wall (beta-lactams) or in protein (macrolides) synthesis has spread worldwide in the last 3 decades (8). The fluoroquinolones (FQs) levofloxacin (LVX) and moxifloxacin are used now for treatment of adult patients with pneumonia. FQ resistance in *S. pneumoniae* is maintained at low prevalence (<3%) in Europe (9, 10), although higher rates have been detected in Asia (11) and in Canada (12). However, an increase in resistance in this bacterium may occur if FQ use is increased (13). FQs target the type II DNA topoisomerases. Despite the functional similarities between topoisomerase IV (topo IV) and gyrase, their susceptibility to FQs varies across bacterial species (14). In *S. pneumoniae*, the primary target for LVX is topo IV (15–18), while gyrase is the primary target for moxifloxacin (19). Type II topoisomerases maintain DNA topology and solve the topological problems associated with DNA replication, transcription, and recombination (20). Gyrase

introduces negative supercoils into DNA (21), whereas topo IV relaxes DNA and participates in chromosome partitioning (22). Chromosomal topology in *Escherichia coli* is maintained homeostatically by the opposing activities of topoisomerases that relax DNA (topo I and topo IV) and by gyrase. In this bacterium, transcription of the *topA* gene encoding topo I increases when negative supercoiling increases (23), while that of *gyrA* and *gyrB* increases after DNA relaxation (24–26). Changes in DNA supercoiling also have a global effect on genome transcription in *E. coli* (27, 28) and *Haemophilus influenzae* (29). We have also shown that relaxation of the *S. pneumoniae* chromosome with novobiocin (NOV; a GyrB inhibitor) causes upregulation of gyrase genes and downregulation of topo I and IV genes and triggers a global transcriptional response affecting ca. 14% of the genome (30). Most (>68%) responsive genes are closely positioned, forming 15 gene clusters (up- and downregulated topological domains), which showed a coordinated response (30).

The killing effect of FQs has been related to the resolution of reaction intermediates of DNA-FQ-topoisomerase complexes, which generates irreparable double-stranded DNA breaks (31).

This could occur in *E. coli* by two pathways, one dependent on protein synthesis and the other independent of it. It has been shown that hydroxyl radical action contributes to FQ-mediated cell death occurring via a protein-dependent pathway (32). This result agrees with a recent proposal suggesting that, following gyrase poisoning, hydroxyl radical formation utilizing internal iron and the Fenton reaction (33) is generated and contributes to cell killing by FQs (34) as well as by other bactericidal antibiotics (35, 36). In this mechanism, proposed for *Enterobacteriaceae* (35, 37), the primary drug interactions stimulate oxidation of NADH via the electron transport chain that is dependent on the tricarboxylic acid cycle. Hyperactivation of the electron transport chain stimulates superoxide formation. Superoxide destabilizes the iron-sulfur clusters of enzymes, making Fe^{2+} available for oxidation by the Fenton reaction. The Fenton reaction leads to the formation of hydroxyl radicals that would damage DNA, proteins, and lipids (38), which results in cell death. Instead of a generalized oxidative damage, a recent study supports that the main action of hydroxyl radicals is the oxidation of guanine (to 8-oxo-guanine) of the nucleotide pool. The incomplete repair of closely spaced 8-oxo-deoxyguanosine lesions caused lethal double-strand DNA breaks, which would underlie much of the cell death caused by beta-lactams and FQs (39). However, recent investigations have questioned the role of hydroxyl radicals and intracellular iron levels in antibiotic-mediated lethality using antibiotic concentrations either similar to (40) or higher than (41) those used previously. The disparate results obtained using diverse antibiotic concentrations and times of treatment emphasize the complexity of the lethal stress response (42).

Given that different antibiotic families have different intracellular targets, it is essential to know the pathway between the initial antibiotic-target interaction and the promotion of hydroxyl radical formation. These pathways are mostly unknown. A model has been proposed for aminoglycosides in *E. coli* whereby the interference of these drugs with ribosome progression would release incomplete polypeptides, which are translocated to the cell membranes, where they may trigger envelope stress. The Arc regulatory system is perturbed, accelerating respiration and thereby increasing the flux of superoxide and hydrogen peroxide into the cell (43). However, for FQs, the specific pathway has not been established, although a general scheme for stress response regulation in *E. coli*, which involves the hydroxyl radical cascade, has been proposed (42). The present study was aimed to understand the transcriptional response to levofloxacin in *S. pneumoniae* at concentrations that inhibited its primary target, topo IV, without inhibiting gyrase, to avoid the opposite effects of these two enzymes on DNA topology. Changes in DNA topology were tested by analyzing the distribution of topoisomers of a replicating plasmid. Global transcription response was analyzed using microarrays technology after cells' exposure to two LVX concentrations. Microarray data were validated by quantitative real-time PCR (qRT-PCR). In addition, transcriptional regulation of the *fatDCEB* operon, coding for an iron transporter, was analyzed. The relation between iron transport and lethality was also tested. Results provide a pathway between topo IV inhibition and hydroxyl radical production and suggest that *S. pneumoniae* uses iron accumulation as part of the death process associated with LVX treatment.

MATERIALS AND METHODS

Bacterial strains and growth and transformation of bacteria. *S. pneumoniae* was grown in AGCH medium with 0.3% sucrose and transformed as described previously (44). MICs of LVX (Sigma) and chloramphenicol (CHL) for strain R6 were 0.25 μg/ml and 1.25 μg/ml, respectively. To construct the Δ*spxB* strain, two fragments of 1,481 bp and 1,374 bp flanking *spxB* were amplified with oligonucleotide pairs SpxBUPF1/SpxBUPR1 and SpxBDOWNF1/SpxBDOWNR1 (see Table S1 in the supplemental material), digested with SphI and XbaI, and ligated to the CHL-acetyl-transferase gene (*cat*) of plasmid pJS3 digested with the same enzymes. R6 was transformed; recombinant colonies were selected in medium containing 2.5 μg/ml CHL and checked by PCR amplification with external oligonucleotides SpxBUPF2/SpxBDOWNR2 (see Table S1 in the supplemental material). Those with the appropriate size (4,574 bp versus 5,352 bp of R6) were sequenced using oligonucleotide CATMED. To construct the R6-P*fat*cat strain, five PCR products were obtained. Two from genes *spr1793* (1,061 bp) and *spr1794* (1,036 bp), flanking the site of insertion, by amplifications with primers 1793F1(XbaI)/spr1793R1 and spr1794F1/spr1794R1(SphI). The third fragment (144 bp) was amplified with UptrcatXba/UptrcatEco and contains the transcriptional terminator that precedes the *cat* cassette in plasmid pJS3. The fourth fragment (422 bp) containing the 5′-upstream region of the iron transport operon *fatDCEB* was amplified with UpfatDF1(EcoRI) and phosphorylated UpFatDR1. The fifth fragment (758 bp) contains *cat* and was amplified with Cat1 phosphorylated and CatDownSph(SphI). Each fragment was digested with the appropriate enzyme, and all fragments were ligated together. The ligation mix was used to transform strain R6, and transformants were selected in medium containing 2.5 μg/ml CHL. This rendered strain R6-P*fat*cat (see Fig. 3A), whose genetic structure was checked by PCR with primers Spr1793R2 and Spr1794F2 and by sequencing with CATMED, CAT191, and spr1793R3.

Analysis of the topology of covalently closed circles. Plasmid DNA isolation from *S. pneumoniae* cultures grown on AGCH medium with 1 μg/ml tetracycline (for pLS1 selection) was performed as described before (30). Circular DNA molecules were analyzed in neutral/neutral two-dimensional agarose gels, which were subjected to Southern hybridization with a 240-bp specific pLS1 probe as described previously (30). DNA linking number (Lk) was calculated by quantifying the amount of every topoisomer. DNA supercoiling density (σ) was calculated from the equation $σ = ΔLk/Lk_0$. Linking number differences (ΔLk) were determined using the equation $Lk = Lk - Lk_0$, in which Lk_0 is $N/10.5$, where N is the size of the molecule (in bp) and 10.5 is the number of base pairs per complete turn in B-DNA.

RNA extraction and real-time RT-PCR experiments. Synthesis of cDNAs from 5 μg of total RNA was performed as previously described (45). These cDNAs were subjected to quantitative qRT-PCR (Chromo 4; Bio-Rad) in 20-μl reaction mixtures containing 2 μl of cDNA, 0.3 μM each specific primer, and 10 μl of LightCycler FastStart Universal A SYBR green Master (Roche). Amplification was achieved with 42 cycles of a tree-segment program: denaturation (30 s at 94°C), annealing (30 s at 45 to 56°C), and elongation (30 s at 68°C). To normalize the three independent cDNA replicate samples, values were divided by those obtained from the amplification of internal fragments of *rpoB* (45) and 16S rRNA genes. The oligonucleotides used are shown in Table S1 in the supplemental material.

Microarray data normalization and analysis. High-density arrays A6701-00-01 from Roche NimbleGen were used. Double-stranded cDNAs were obtained from total RNA with the SuperScript Double-Stranded cDNA Synthesis kit (Invitrogen). Labeling of cDNAs with Cy3 and hybridization were performed at the Institut de Recerca Biomèdica, Barcelona (Spain). A GenePix 4000B scanner at 5-μm resolution was used, and raw data were extracted and robust multiarray average (RMA) normalized using NimbleScan v2.4. After this normalization, Partek Genomics Suite 6.4 was used to do a principal component analysis and test for significance for differential gene expression using analysis of variance

(ANOVA). Each microarray experiment was carried out in duplicate with cDNA prepared from two independent cultures.

Detection of reactive oxygen species. The intracellular oxidation levels were measured using dihydrorhodamine 123 dye (Sigma-Aldrich), a nonfluorescent compound that diffuses passively across membranes. Oxidation converts it to the fluorescent product rhodamine 123, and this fluorescence is proportional to the level of oxidation (37). In a typical experiment, cells were grown exponentially to an optical density at 620 nm (OD_{620}) of 0.4 before LVX was added. One-milliliter samples were collected, and cells were washed once in 500 μl of 1$\times$ phosphate-buffered saline (PBS) (pH 7.2), suspended in 250 μl of 1$\times$ PBS containing 2.5 μg/ml of dihydrorhodamine 123, and incubated at 37°C in the dark for 30 min. Cells were washed once in 500 μl of 1$\times$ PBS and suspended in 250 μl of 1$\times$ PBS. A volume of 200 μl was used to measure fluorescence. The fluorescence signal was analyzed using a Tecan Infinite 2000 with excitation wavelength (λ)/emission λ of 485 nm/535 nm. Results were expressed as relative fluorescence units (RFU) and were normalized according to the number of live cells at each time point (46).

Microarray data accession number. All microarray data are available at the Array Express (EBI, United Kingdom) database via accession number E-MEXP-3809.

RESULTS

DNA topoisomer distribution did not vary under treatment with LVX. The effect of LVX was tested in the reference strain R6 carrying plasmid pLS1 at subinhibitory (0.5$\times$ MIC) and fully inhibitory (10$\times$ MIC) concentrations. The change in OD_{620} along the 60 min of the experiment was from 0.4 to 0.8. Cell division was inhibited only when the culture was treated with LVX at 10$\times$ MIC, with decreases in cell viability to about 70% and 97% at 30 and 60 min, respectively (Fig. 1A). To measure supercoiling alterations, topoisomer distributions of the replicating pLS1 plasmid were analyzed. Under the chloroquine concentration used, the induced ΔLk is −14 (30). Topoisomers appeared distributed in the autoradiograms in a bubble-shaped arc, where negative and positive supercoiled molecules are located to the right and to the left sides, respectively (Fig. 1B). Although we have not measured the supercoiling level of the bacterial chromosome, the values obtained on small plasmids provide a good estimation of chromosomal supercoiling (47). No significant differences in supercoiling densities (σ) were detected under any condition, showing that the inhibition of topo IV by LVX did not have a detectable effect in the level of global supercoiling and that gyrase was not inhibited at the LVX concentrations used.

Two kinds of transcriptional responses in LVX-treated cultures: growth related and LVX related. The transcriptional response was measured in cultures of strain R6 at three time points (5, 15, and 30 min) after treatment with LVX concentrations of 0.5$\times$ MIC and 10$\times$ MIC. In addition, samples taken at 15 and 30 min of an untreated culture (No-LVX) were also analyzed and used to distinguish those genes varying along the growth curve. Only gene expression variations $\geq$2 (P values < 0.01) with respect to time zero min were considered. The whole transcriptomic response is shown in Table 1. Based on the results obtained, responsive genes were classified into two categories: growth related and LVX related (Fig. 2; Table 1). Growth-related genes included 108 genes showing transcription variations in the No-LVX culture. Additionally, 10 genes forming parts of operons with these genes were also considered to be growth related. In total, 118 genes (5.8% of the genome) showed variations associated with growth (Fig. 2A).

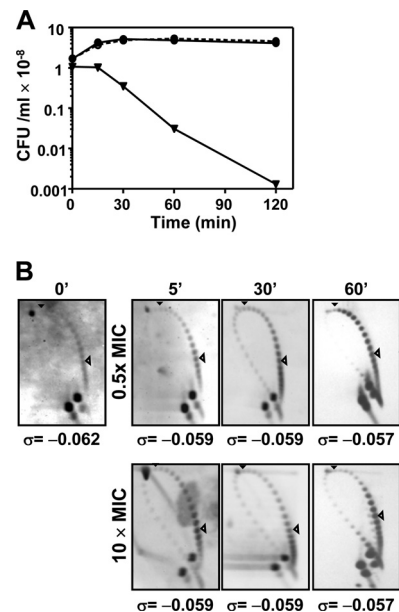Genes controlled by two-component system 12 (TCS-12) and

FIG 1 Global supercoiling did not vary under treatment of *S. pneumoniae* R6 (pLS1) with levofloxacin. (A) Viability. (B) Topoisomer distribution of pLS1. Exponentially growing cultures in AGCH at OD_{620} of 0.4 were treated with the indicated LVX concentrations. Values of a typical experiment are indicated. Samples were taken before the addition of the drug (time zero min), and at the indicated times, plasmid DNA was isolated and subjected to two-dimensional agarose gel electrophoresis run in the presence of 1 and 2 μg/ml chloroquine in the first and second dimensions, respectively. Supercoiling density (σ) values are indicated. A black arrowhead indicates the topoisomer that migrated with ΔLk of 0 in the second dimension and has a ΔWr of −14. An open arrowhead points to the more abundant topoisomer.

TCS-13 represented the greatest proportion (50.8%) of responsive genes (Table 1; Fig. 2C). TCS-12 regulates competence for genetic transformation (48). The regulatory cascade begins with the secretion and processing of ComC by the dedicated ABC transporter ComAB. Processed ComC activates TCS-12 ComDE: ComD is the histidine kinase (that senses the stimulus), and ComE is the response regulator (the transcriptional modulator of the responsive genes). Phosphorylated ComE activates the transcription of early genes, including the alternative sigma factor ComX (49), which activates transcription of late competence genes (50, 51). Among competence genes, 53 (11 early and 42 late genes) showed downregulation. These included most (10 of 18) genes of the early competence response (50), which are transcribed from 7 of the 10 promoters (Table 1) containing the binding site of the transcriptional activator ComE (52). Early downregulated genes included those coding for the two transcriptional regulators of competence, *comE* and two genes coding for the alternative sigma factor ComX (53), required for induction of many late genes. In accordance, 42 of the 81 late-competence genes (50) were downregulated. These 42 genes were transcribed from 13 of 19 promoters containing a ComX box. Concerning TCS-13 (SpiRH), 13 genes containing regulatory sequences for its response regulator SipR (54, 55) were upregulated, including *spiP* encoding the bacteriocin with a Gly-Gly motif and the dedicated ABC transporter (*spiABCD*).

The LVX-related response involved 108 of 174 genes that did not show variations in the No-LVX culture (Fig. 2B). Of them, 4 varied only at 5 min after 10$\times$ MIC treatment. Among LVX-re-

TABLE 1 Genes involved in the transcriptomic response of *S. pneumoniae* R6 to levofloxacin (LVX)[a]

Role or subrole	R6 locus (gene)	Mean relative fold change[b]							
		No LVX		LVX at 0.5× MIC			LVX at 10× MIC		
		15 min	30 min	5 min	15 min	30 min	5 min	15 min	30 min
Amino acid biosynthesis	spr0515 (*metF*)	—	−2.3	—	—	−2.1	—	—	—
Biosynthesis of cofactors	spr0636	—	—	—	—	—	2.0	—	—
	spr1438 (*entB*)	—	—	—	—	—	—	—	−2.2
Cell envelope	spr0867 (*lytB*)	**2.9**	**2.5**	—	**3.6**	**2.7**	—	**3.5**	**3.2**
	spr1324 (*apbE*)	—	—	—	—	—	—	—	−2.1
TCS12/ComCDE (°ComE box)	spr0013° (*comX1*)	—	−7.8	—	—	—	—	—	—
	spr0020° (*comW*)	—	−2.5	—	—	—	—	—	—
	spr0043*°-0044 (*comAB*)	—	−3.5	—	—	—	—	—	—
	spr1017° (*mreA*)	—	−3.0	—	—	—	—	—	—
	spr1819° (*comX2*)	—	−7.8	—	—	—	—	—	—
	spr1762°	—	−6.0	—	—	−2.0	—	—	—
	spr2043*°-2041 (*comC*)	—	−8.8	—	—	−2.4	—	—	—
(°°ComX box)	spr0027°°	—	−2.8	—	—	—	—	—	—
	spr0031*°°-0030	—	−4.8	—	—	−3.0	—	—	—
	spr0128*°°-0127 (*cibA*)	—	−2.7	—	—	−2.2	—	—	—
	spr0181°° (*orf47*)	—	−3.6	—	—	−	—	—	—
	spr0856*°°-0860 (*comEA-EC*)	—	−6.9	—	—	−2.2	—	—	—
	spr0881°° (*coiA*)	—	−8.3	—	—	−2.7	—	—	—
	spr0996°° (*radC*)	—	−6.6	—	—	−2.3	—	—	—
	spr0997	—	−3.9	—	—	—	—	—	—
	spr1144 (*dprA*)	—	−5.3	—	—	−2.1	—	—	—
	spr1628*°°-1631 (*cclA*)	—	−4.5	—	—	−2.6	—	—	—
	spr1758*°°-1756 (*cinA-recA-dinF*)	—	−3.1	—	—	—	—	—	—
	spr1831*°°-1826	—	−9.2	—	—	−3.0	—	—	−2.1
	spr1864*°°-1855 (*cglABCDFG*)	—	−2.5	—	—	—	—	—	—
	spr2006°° (*cbpD*)	—	−6.2	—	—	−2.4	—	—	—
	spr2013*°°-2012 (*comF-FC*)	—	−11.9	—	—	−3.0	—	—	—
TCS13/SpiRH (●SpiR box)	spr0040● (*pncE*)	—	**2.7**	—	—	**2.2**	—	—	**2.0**
	spr0461●	—	**2.1**	—	—	**2.9**	—	—	**2.7**
	spr0469*●-0465 (*spiABCDP*)	—	**2.4**	—	**2.2**	**3.3**	—	—	**2.5**
	spr0470*●−0475 (*pncW*)	—	**3.1**	—	**2.2**	**4.1**	—	—	**3.2**
Pathogenesis	spr0121 (*pspA*)	—	—	—	—	—	—	—	−2.6
	spr0328 (*eng*)	—	—	—	—	—	—	—	−2.1
	spr0565 (*bgaA*)	—	—	—	—	—	—	—	−2.6
	spr1652*-1649 (*pfbA*)	—	—	—	—	—	—	—	−2.4
Central metabolism	spr1867 (*nagA*)	—	—	—	—	—	—	—	−2.5
	spr1833 (*bgl2*)	—	—	—	—	—	—	—	−2.2
	spr1285*-1287	—	—	—	—	—	—	—	−2.3
	spr1666 (*dpnD*)	—	—	—	2.0	—	—	2.1	—
Energy metabolism	spr1029 (*glgB*)	—	—	—	—	2.1	—	—	2.2
	spr0226 (*pflE*)	—	—	—	—	—	—	—	−2.2
	spr1837 (*adhE*)	—	—	—	—	—	−2.2	—	—
	spr0064 (*agaS*)	—	—	—	—	—	2.0	—	−2.5
	spr1028 (*gapN*)	—	—	—	—	—	−2.5	—	—
	spr0065 (*galM*)	—	—	—	—	—	—	—	−2.2
	spr0276	—	—	—	—	3.8	—	—	3.7
	spr1647*-1648 (*galET*)	—	—	—	—	—	—	−2.0	−3.2
	spr1668*-1667 (*galK*)	—	2.7	—	—	—	—	—	—
	spr1974 (*fcsR*)	—	—	—	—	—	—	−2.0	−4.1
Protein fate	spr1204 (*ptrB*)	—	—	—	—	2.0	—	—	—
Ribosomal proteins synthesis	spr0078 (*rpsD*)	—	—	—	—	—	—	—	−2.1
	spr1211 (*rplL*)	—	—	—	—	—	—	—	−2.4
	spr0682 (*rpsP*)	—	—	—	—	—	—	—	−2.4
	spr1271 (*rpsU*)	—	—	—	—	—	—	—	−2.1
	spr1943*-1944 (*rpmFG*)	—	—	—	—	—	—	—	−2.0

(Continued on following page)

TABLE 1 (Continued)

Role or subrole	R6 locus (gene)	Mean relative fold change[b]							
		No LVX		LVX at 0.5× MIC			LVX at 10× MIC		
		15 min	30 min	5 min	15 min	30 min	5 min	15 min	30 min
Purines, pyrimidines, nucleosides, and nucleotides	spr0045*-0055 (pur, van, pyr)	**8.0**	**8.1**	—	**16.9**	**15.1**	—	**16.2**	**11.2**
	spr0613*-0614	**2.6**	—	—	**3.8**	**2.4**	—	**3.6**	**2.8**
	spr0865*-0866 (pyrDIID)	—	—	—	**2.5**	**2.0**	—	**2.6**	**2.4**
	spr1153 (carB)	—	—	—	**2.1**	**2.1**	—	**2.0**	—
	spr1662*-1663 (xpt, pbuX)	—	—	—	**2.8**	**3.8**	—	**3.1**	**2.8**
	spr1709 (gtfA)	—	−2.9	—	—	—	—	—	—
Transcription	spr0634	—	—	—	—	—	**2.0**	—	—
	spr0227 (deoR)	—	—	—	—	—	—	—	−2.4
	spr0279 (bglG)	—	—	—	**3.2**	**4.1**	—	—	**3.8**
	spr1067 (lacR)	—	—	—	—	—	—	—	−2.1
	spr1439 (codY)	—	—	—	—	—	—	—	−2.0
	spr1889	—	—	—	—	—	—	—	−2.8
	spr1899 (phoU)	−2.3	−2.3	—	—	—	—	—	—
	spr1933 (rgg)	—	−3.2	—	—	—	—	—	—
Transport and binding	spr0551 (brnQ)	—	—	—	—	—	**2.3**	—	**2.1**
	spr0624*-0622 (glnQ)	—	—	—	—	—	—	**2.1**	**2.1**
	spr1895*-1898	−2.4	−2.2	—	—	—	—	—	—
	spr1641 (ctpA)	—	—	—	—	—	—	−2.4	−2.9
	spr1684*-1687 (fatDCEB)	—	—	**3.7**	**4.7**	**3.3**	**3.8**	**6.2**	**5.6**
	spr0264*-0265	—	—	—	**3.0**	**2.9**	—	**3.0**	**2.0**
	spr0278	—	—	—	—	**5.2**	—	—	**4.7**
	spr0280	—	—	—	**2.4**	**2.6**	—	—	**2.6**
	spr1710	—	−2.0	—	—	—	—	—	—
	spr1834*-1836 (ptcAB)	—	—	—	—	—	—	—	−2.2
	spr0081	—	—	—	**2.0**	—	—	—	—
	spr0619	**2.5**	**2.9**	—	**2.2**	**2.2**	—	**2.3**	**2.0**
	spr0621*-0620	—	—	—	**2.0**	**2.0**	—	**2.3**	**2.2**
	spr1097 (nirC)	**2.2**	**2.1**	—	—	—	—	—	—
	spr1202	—	**2.1**	—	—	—	—	—	—
	spr1203	—	**2.1**	—	—	**2.4**	—	—	—
	spr1381*-1378	**2.1**	—	—	**2.2**	—	—	—	—
	spr1441 (oxlT)	—	—	—	**3.0**	**4.3**	**2.2**	**3.5**	**4.0**
	spr1546	—	**3.7**	—	—	—	—	—	—
	spr1646*-1643	—	—	—	—	—	—	—	−2.1
	spr1801	—	—	—	**3.0**	**2.8**	−	**3.4**	**2.4**
	spr1817	—	—	—	−2.0	—	—	—	—
Unclassified	spr0907*-0908 (phtDE)	—	—	—	—	—	—	—	−2.8
	spr1060 (phpA)	—	—	—	—	—	—	—	−2.2
Transposon functions	spr0018	—	—	—	—	−2.3	—	—	—
	spr0019	—	—	—	—	−2.2	—	—	—
	spr0041	—	—	—	—	**3.1**	—	—	**2.7**
	spr0612	—	—	—	—	—	—	**2.5**	—
	spr0273	—	−2.6	—	—	—	—	—	—
	spr1349*-1347	−2.4	−2.0	—	−2.0	—	—	—	—
	spr1367	−2.4	−2.3	—	—	—	—	—	—
	spr1563	—	—	—	—	−2.0	—	—	—

[a] The responsive genes included showed significant fold variations (≥2 and $P < 0.01$). All genes showing variations, with the exception of 47 encoding hypothetical proteins, are included. Genes considered to be involved in the LVX-mediated transcriptomic response (i.e., that did not show variations in the no-LVX culture) are shaded in gray. Nonshaded genes are considered to be involved in the growth-related response. Symbols: *, the first gene of the putative operon; °, gene with a ComE box; °°, gene with a ComX box; ●, gene with a SpiR box; —, no change.

[b] In operons, values indicated correspond to those of the first gene of the operon, except in spr0045-0055, spr0613-0614, spr1859-1898, and spr1864-1855, in which variations corresponded to the second gene. Values above 2 are shown in boldface.

sponsive genes, 24.1% code for hypothetical proteins, and the same proportion code for transport proteins (Fig. 2C). Interestingly, the only genes upregulated at 5 min in 0.5× MIC were the four genes of the *fatDCEB* operon (56). These genes were upregulated at every time and LVX concentration used. We have previ-

ously shown that the *fatDCEB* operon is located in a topological domain, D14 (Fig. 3A), showing downregulation under NOV treatment, as tested by microarray experiments (30). We validated these results by qRT-PCR, showing that treatment with NOV caused a decrease in *fatD* transcription at any time tested at 10×
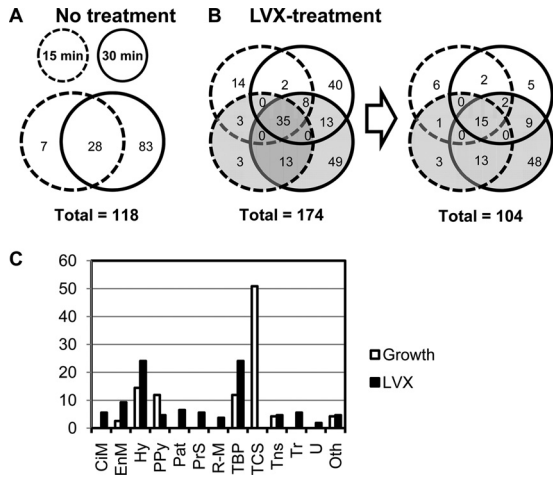
FIG 2 Gene expression analysis under the three conditions assayed. (A and B) Responsive genes represented in Venn diagrams with 3 circles, each one corresponding to one time interval under each condition, showing the differentially expressed genes in microarrays. (B) All genes (left diagram) or only those genes that differed from those present in the No-LVX sample (right diagram) are indicated. A complete list of these genes can be found in Table 1. (C) Classification of responsive genes by functional classes: CiM, central intermediary metabolism; EnM, energy metabolism; Hy, hypothetical proteins; PPy, purines, pyrimidines, nucleosides, and nucleotides; Pat, pathogenesis; PrS, protein synthesis; R-M, restriction-modification; TBP, transport and binding proteins; TCS, two-component systems; Tns, transposon functions; Tr, transcription; U, unclassified; Oth, other (classes with a representation of <2%).

MIC and at 5 min at 0.5× MIC. At 0.5× MIC, a recovery in *fatDCE* transcription was observed (Fig. 3B), as expected from the general supercoiling recovery (30). In contrast, qRT-PCR confirmed the upregulation of *fatDCEB* at all times regardless of LVX concentration (Fig. 3C), with fold variation values similar to those in microarrays. To test the role of topo IV inhibition in the upregulation of *fatD*, qRT-PCR determinations in an LVX-resistant R6 mutant containing a ParCS79F change in topo IV (45), treated with the same LVX concentrations that R6, were performed. No increase of *fatD* transcription in this strain was observed.

fatDCEB transcription is affected by supercoiling levels. Even when no changes in the general supercoiling levels were detected in the presence of LVX (Fig. 1C), we assumed that local changes in supercoiling could be involved in the regulation of the *fatDCEB* operon. To check this possibility, a strain (R6-P$_{fat}$cat [Fig. 3A]) that contains a 422-bp region located upstream of *fatDCEB* that includes the promoter of the operon (P$_{fat}$), fused to the *cat* reporter gene, was inserted into the chromosome 106 kb away from *fatDCEB* (Fig. 3A). The levels of transcription of *fatD* and *cat* were tested by qRT-PCR in cultures treated with two LVX concentrations (Fig. 3C). While *fatD* showed upregulation in the presence of LVX, almost no change was observed in *cat* transcription. Thus, supercoiling alteration induced by LVX is acting as a regulator of P$_{fat}$, given that its transcriptional upregulation is dependent on its location in a topological chromosomal domain.

In addition, the level of transcription of *fatDCEB* was tested by qRT-PCR in cultures treated either with NOV, an inhibitor of
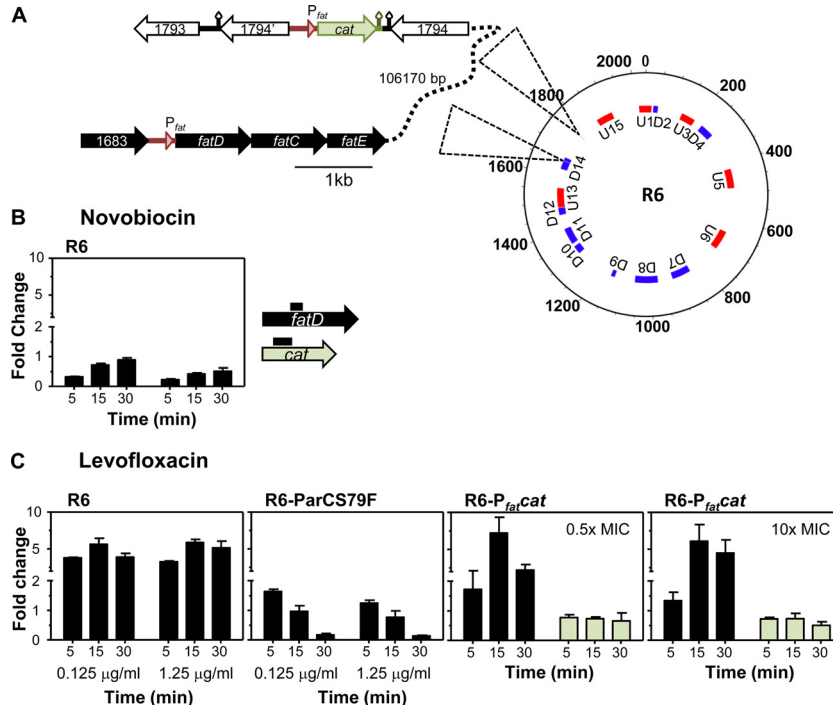
FIG 3 Transcription of *fatD* depended on the inhibition of topoisomerase IV by LVX. (A) Genetic structure of strain R6-P$_{fat}$cat showing the chromosomal location of P$_{fat}$*fatDCEB* and P$_{fat}$*cat*. Topology-reacting gene clusters detected after DNA relaxation with NOV are indicated: U1 to U15, upregulated domains; D1 to D14, downregulated domains. (B) Transcriptional response after NOV treatment measured by qRT-PCR on exponentially growing cultures of strain R6. (C) Transcriptional response of R6, of an LVX-resistant derivative (R6-ParCS79F), and of strain R6-P$_{fat}$cat. Cultures were grown in AGCH to an OD$_{620}$ of 0.4 and treated with LVX at 0.125 µg/ml LVX (0.5× MIC of R6 and R6-P$_{fat}$cat; 0.05× MIC of R6-ParCS79F) and at 2.5 µg/ml LVX (10× MIC of R6 and R6-P$_{fat}$cat; 0.5× MIC of R6-ParCS79F). Total RNA was isolated; cDNA was synthesized and subjected to qRT-PCR. Data were normalized to time zero min. Transcription represented the means of qRT-PCR values of three independent replicates ± standard errors of the means (SEM).
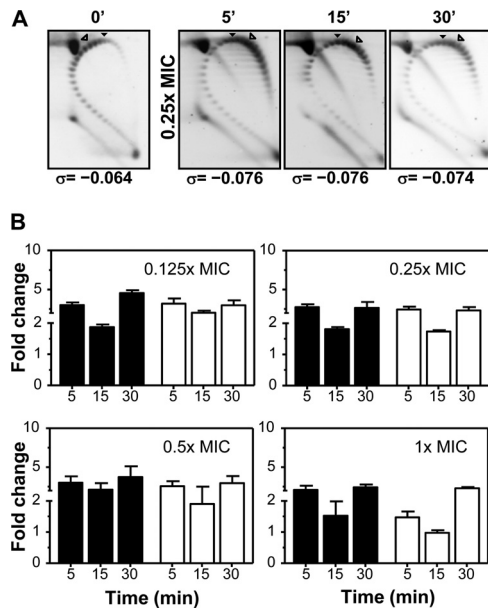
FIG 4 Transcription of *fatD* depended on the general supercoiling level. Cultures were grown as indicated in the legend to Fig. 3 and treated with *N*-methyl-seconeolitsine at the indicated concentrations. (A) Plasmid DNA was isolated at the indicated times and subjected to two-dimensional agarose gel electrophoresis in the presence of 5 and 15 μg/ml chloroquine in the first and second dimensions, respectively. Supercoiling density (σ) values are indicated. A black arrowhead indicates the topoisomer that migrated with ΔLk of 0 in the second dimension that has a ΔWr of −30 (58). An open arrowhead indicates the more abundant topoisomer. (B) Total RNA was isolated; cDNA was synthesized and subjected to qRT-PCR, and *fatD* (black bars) and *fatC* (white bars) values were normalized to time zero min. Transcription represented the means of qRT-PCR values of three independent replicates ± SEM.

GyrB (21, 57) (Fig. 3B), or with *N*-methyl-seconeolitsine (a topo I inhibitor) (58). Treatment with *N*-methyl-seconeolitsine caused, as expected (58), a general increase in supercoiling (Fig. 4A). This increase was accompanied by a rise in the transcription of *fatD* and *fatC* at every concentration tested (Fig. 4B).

Transcriptional activation of iron transport induced by LVX is involved in cell death. The increase in transcription of the *fatDCEB* operon would lead to the accumulation of toxic concentrations of iron within the cell. This toxicity would be related to the activation of the Fenton reaction, which utilizes unincorporated intracellular iron and transfers an electron to hydrogen peroxide (Fig. 5A). To test if intracellular iron is an important component of the LVX-mediated killing, R6 was grown in the presence of LVX in three different media: AGCH (containing 1.58 μM SO_4Fe), AGCH plus the iron chelator *o*-phenanthroline, or AGCH deficient in SO_4Fe (AGCH*). Attenuation of the bactericidal effect of LVX, both in AGCH + *o*-phenanthroline and in AGCH*, was observed, suggesting a role for intracellular iron in LVX lethality (Fig. 5B).

The main source of endogenous hydrogen peroxide in *S. pneumoniae* is SpxB (59), the pyruvate oxidase enzyme (EC 1.2.3.3) that decarboxylates pyruvate to acetyl phosphate plus H_2O_2 and CO_2 (Fig. 5A). To assess that LVX lethality was related to the production of hydroxyl radicals via the Fenton reaction, an SpxB deletion mutant was constructed as detailed in Materials and Methods. The Δ*spxB* strain was less susceptible to the killing by LVX, the attenuation being similar to that exhibited by R6 grown either in the presence of *o*-phenanthroline or in AGCH* (Fig. 5B).
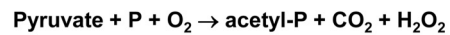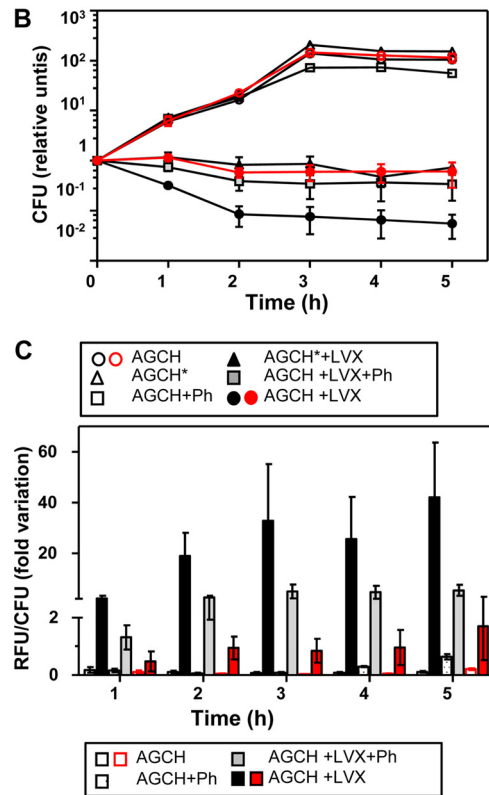


FIG 5 LVX lethality is related to the level of intracellular iron. (A) Enzymatic reaction of SpxB that renders H_2O_2, a substrate of the Fenton reaction. P, phosphate. (B) Viability of *S. pneumoniae* R6 (black symbols) or R6-Δ*spxB* (red symbols) either in AGCH, in AGCH plus the iron chelator *o*-phenanthroline (AGCH+Ph), or in AGCH deficient in SO_4Fe (AGCH*). Cultures were grown in AGCH to an OD_{620} of 0.4, diluted 100-fold, and treated, when indicated, with LVX at concentrations equivalent to 2.5× MIC. (C) Accumulation of reactive oxygen species. Results are the means ± SEM of three independent replicates. RFU, relative fluorescence units; values were made relative to zero min and divided by the number of viable cells.

These results provided a relation between LVX lethality and the Fenton reaction via the increase of intracellular iron. In addition, accumulation of reactive oxygen species was measured by the oxidation of dihydrorhodamine 123. Accumulation was observed in R6 cultures treated with LVX (Fig. 5C), with increases with respect to time zero min higher than 35-fold at 3, 4, and 5 h of treatment. Similar increases in reactive oxygen species had been observed in ciprofloxacin-treated *S. pneumoniae* with a different dye probe (46) and also in norfloxacin-treated *E. coli* (35). This accumulation was reverted about 10-fold by *o*-phenanthroline. A similar reversion was observed in the Δ*spxB* strain.

DISCUSSION

The complex transcriptional response observed in our microarray experiments led us to differentiate among those genes whose transcription was altered as a consequence of growth and those that
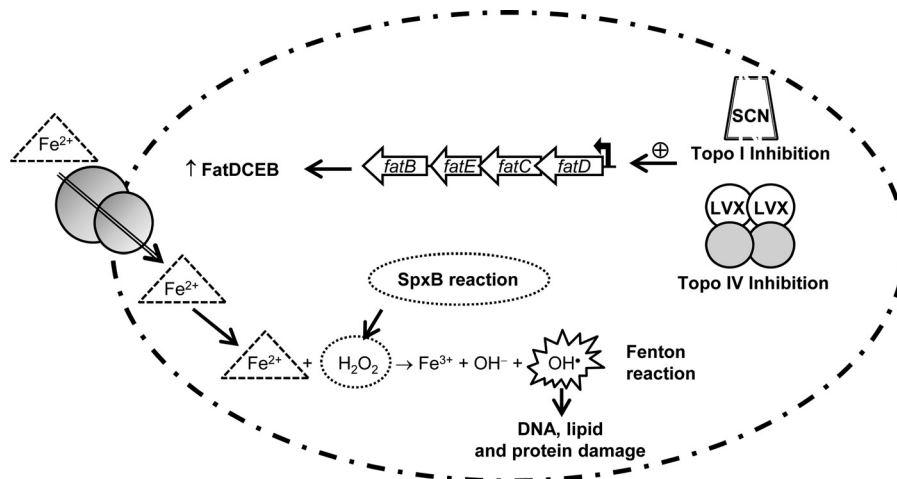
FIG 6 Oxidative damage cell death pathway. The inhibition of topo IV by levofloxacin (LVX) or of topoisomerase I by *N*-methyl-seconeolitsine (SCN) would cause a local increase in supercoiling resulting in the upregulation of the *fatDCEB* operon. The consequent increase in this iron transporter causes an increase of intracellular ferrous iron (Fe^{2+}). This compound and hydrogen peroxide (produced by the activity of the SpxB pyruvate oxidase) are the substrates of the Fenton reaction. The Fenton reaction renders hydroxyl radicals, which oxidatively damage DNA, proteins, and lipids.

were LVX dependent. We detected that 5.8% of the genome varied as a consequence of growth, involving mainly genes of 2 of the 13 pneumococcal two-component systems, TCS-12 and TCS-13. The major response corresponded to genes dependent on TCS-12 (ComDE), involved in the regulation of competence for genetic transformation. However, in the presence of LVX, competence genes showed decreases in transcription lower (2.7 ± 0.8, average ± standard deviation [SD]) than those observed at 30 min in the untreated culture. These results suggest that two opposed regulation mechanisms are acting over competence development in the LVX-treated cultures: the growth phase caused downregulation of competence genes, while LVX counteracted this downregulation. These results are in agreement with the described transcriptional activation of *ssbB*, a late competence gene, after 2.5 h of FQ treatment, with the subsequent induction of transformability (60). Thus, in response to FQs, *S. pneumoniae*, a bacterium lacking an SOS-like system, activates the competence regulon, supporting the hypothesis that competence is a general stress response of *S. pneumoniae* (60). Conversely, the upregulation of the genes controlled by TCS-13 (SpiRH) was not affected by LVX treatment.

The LVX-related response included 108 genes (5.2% of the genome). The most striking result in the LVX response was the upregulation of the *fatDCEB* operon at the earliest time analyzed (5 min) and at the subinhibitory (0.5× MIC) concentration, being the only genes varying under this condition. We tested *fatD* transcription in an LVX-resistant R6 mutant, and no upregulation was observed in the presence of the antibiotic (Fig. 3C). These results indicate that the LVX transcriptional effects were indeed due to the inhibition of topo IV. However, changes in the general supercoiling levels in the presence of LVX were not found (Fig. 1C). Likewise, no changes in general chromosomal supercoiling were observed in *E. coli* cells treated with oxolinic acid, an inhibitor of gyrase (61).We assumed that local changes in supercoiling could be involved in the regulation of *fatDCEB*. To test the role of supercoiling in *fatDC* transcription, we altered global supercoiling in both directions. On one side, we increased global supercoiling by using the DNA topo I inhibitor *N*-methyl-seconeolitsine (58). On the other, we decreased supercoiling by using the gyrase B

inhibitor NOV (57). We observed an increase both in supercoiling (Fig. 4A) and in *fatDC* transcription with the topo I inhibitor (Fig. 4B). In contrast, treatment with NOV caused a decrease in *fatDC* transcription, as detected by qRT-PCR (Fig. 3B), in accordance with a general supercoiling decrease and downregulation of *fatDCE* transcription in microarrays (30). Microarray results have shown that *fatDCEB* is located in topological cluster D14, which contains genes downregulated when DNA supercoiling decreases (30). We constructed a strain with a copy of the 422-bp *fatDCEB*-upstream region fused to *cat* inserted 106 kb away from its native position. Transcription from P_{fat} in the presence of LVX varied depending on its chromosomal location. It was upregulated in its appropriate chromosomal location in downregulated cluster D14 but was almost not regulated when located 106 kb away (Fig. 3), in a nonregulated domain.

Besides this supercoiling regulation, the *fatDCE* operon has been shown to be regulated in several ways, as expected for an operon essential for iron homeostasis. Among them, environmental factors, such as high levels of extracellular Mn^{2+} (62) and low pH (63) caused its transcriptional upregulation, whereas aerobiosis caused its downregulation (64). Other regulators of the operon are the RitR repressor and (56) the CodY repressor, whose DNA binding capacity is modulated by branched-chain amino acids (65, 66). In accordance, we observed *codY* downregulation in the LVX response (Table 1), probably contributing to the upregulation of *fatDCEB*.

The genome of *S. pneumoniae* R6 encodes three operons for iron transport systems (spr0224-spr0220, spr0934-spr0936, and *fatDCEB*). Of these, only *fatDCEB* is involved in iron (Fe^{2+} and Fe^{3+}) uptake (67). In this way, the upregulation of the operon would cause an increased uptake of iron and its intracellular accumulation, which in turn would activate the Fenton reaction (Fig. 5A). We have observed attenuation of the LVX bactericidal effect in media defective in iron (Fig. 5B), confirming that intracellular iron is a component of LVX-mediated killing. In addition, the accumulation of reactive oxygen species (Fig. 5C) was in accordance with this interpretation. These results agree with the proposed mechanism of killing by bactericidal antibiotics, includ-

ing FQs (35). The stimulation of the Fenton reaction is the final common step. However, there are several differences between this model and the one we propose in this study (Fig. 6). *S. pneumoniae* is a lactic acid bacterium that obtains its metabolic energy exclusively from the fermentation of carbohydrates via glycolysis. Its genome does not contain genes for the tricarboxylic acid cycle and lacks the cytochromes and heme-containing proteins involved in aerobic respiration. In addition, although genes coding the F_oF_1-ATPase are present, this proton pump does not synthesize ATP; conversely, it works at the expense of ATP and serves as the major regulator of intracellular pH (68). Consequently, the only enzymes annotated as iron-sulfur dependent in the *S. pneumoniae* R6 genome are the two subunits of the L-Ser dehydratase (Spr0094 and Spr0095). The main reason for the increase of intracellular Fe^{2+} in the presence of LVX should be transcriptional activation of the *fatDCEB* transporter. The importance of iron in the susceptibility to antibiotics has been recently reinforced by the demonstration that overexpression of an iron efflux system in *Salmonella enterica* serovar Typhimurium protects cells against ampicillin and ciprofloxacin (69). With respect to the other component of the Fenton reaction—hydrogen peroxide—it is produced in *S. pneumoniae* mainly by the SpxB enzyme (59, 70). We deleted the gene encoding this enzyme (*spxB*) and observed that the mutant strain was more resistant to the killing by LVX than its *spxB*⁺ parental strain, the attenuation being similar to that exhibited by R6 grown in iron-deficient media (Fig. 5B). The difference in lethality between the wild-type R6 strain and the R6-Δ*spxB* mutant in the presence of 2.5× MIC LVX was in the same range as that observed between *E. coli* wild-type and mutant strains lacking either superoxide dismutase activities (36) or both catalase and peroxidase activities (36, 40), which accumulate H_2O_2, in the presence of norfloxacin at 4× to 10× MIC. We have observed protection to FQ lethality using low LVX concentrations (2.5× MIC), in agreement with results of *E. coli* treatment with norfloxacin at 2× to 4× MIC (41). In conclusion, we have shown for the first time that *fatDCEB* transcription is regulated by the supercoiling level. The primary effect of the interaction of LVX-topo IV is the upregulation of the operon by local increase in DNA supercoiling. This upregulation would increase the intracellular level of iron, which activates the Fenton reaction, increasing the concentration of hydroxyl radicals. These effects were observed before the inhibition of protein synthesis mediated by LVX. All these effects, together with the DNA damage caused by the inhibition of topo IV, would account for LVX lethality. The possibility to increase FQs' efficacy by elevating the levels of intracellular ferrous iron remains open.

ACKNOWLEDGMENTS

REFERENCES

1. **World Health Organization.** 2007. Pneumococcal conjugate vaccine for childhood immunization—WHO position paper. Wkly. Epidemiol. Rec. **82:**93–104. http://www.who.int/wer/2007/wer8212.pdf.
2. **Whitney CG, Farley MM, Hadler J, Harrison LH, Bennett NM, Lynfield R, Reingold A, Cieslak PR, Pilishvili T, Jackson D, Facklam RR, Jorgensen JH, Schuchat A, the Active Bacterial Core Surveillance of the Emerging Infections Program Network.** 2003. Decline in invasive pneumococcal disease after the introduction of protein-polysaccharide conjugate vaccine. N. Engl. J. Med. **348:**1737–1746. http://dx.doi.org/10.1056/NEJMoa022823.
3. **Kyaw MH, Lynfield R, Schaffner W, Craig AS, Hadler J, Reingold A, Thomas AR, Harrison LH, Bennett NM, Farley MM, Facklam RR, Jorgensen JH, Besser J, Zell ER, Schuchat A, Whitney CG, Active Bacterial Core Surveillance of the Emerging Infection Program Network.** 2006. Effect of introduction of the pneumococcal conjugate vaccine on drug-resistant *Streptococcus pneumoniae.* N. Engl. J. Med. **354:**1455–1463. http://dx.doi.org/10.1056/NEJMoa051642.
4. **Pilishvili T, Lexau C, Farley MM, Hadler J, Harrison LH, Bennett NM, Reingold A, Thomas A, Schaffner W, Craig AS, Smith PJ, Beall BW, Whitney CG, Moore MR, the Active Bacterial Core Surveillance/ Emerging Infection Program Network.** 2010. Sustained reductions in invasive pneumococcal disease in the era of conjugate vaccine. J. Infect. Dis. **201:**32–41. http://dx.doi.org/10.1086/648593.
5. **Fenoll A, Granizo JJ, Aguilar L, Gimenez MJ, Aragoneses-Fenoll L, Hanquet G, Casal J, Tarragó D.** 2009. Temporal trends of invasive *Streptococcus pneumoniae* serotypes and antimicrobial resistance patterns in Spain from 1979 to 2007. J. Clin. Microbiol. **47:**1012–1020. http://dx.doi.org/10.1128/JCM.01454-08.
6. **Fenoll A, Gimenez MJ, Vicioso MD, Granizo JJ, Robledo O, Aguilar L.** 2009. Susceptibility of pneumococci causing meningitis in Spain and prevalence among six isolates of serotypes contained in the 7-valent pneumococcal conjugate vaccine. J. Antimicrob. Chemother. **64:**1338–1340. http://dx.doi.org/10.1093/jac/dkp376.
7. **Moore MR, Gertz JRE, Woodbury RL, Barkocy-Gallagher GA, Schaffner W, Lexau C, Gershman K, Reingold A, Farley M, Harrison LH, Hadler JL, Bennett NM, Thomas AR, McGee L, Pilishvili T, Brueggemann AB, Whitney CG, Jorgensen JH, Beall B.** 2008. Population snapshot of emergent *Streptococcus pneumoniae* serotype 19A in the United States, 2005. J. Infect. Dis. **197:**1016–1027. http://dx.doi.org/10.1086/528996.
8. **Jacobs MR, Felmingham D, Appelbaum PC, Grüneberg RN, the Alexander Project Group.** 2003. The Alexander Project 1998–2000: susceptibility of pathogens isolated from community-acquired respiratory tract infection to commonly used antimicrobial agents. J. Antimicrob. Chemother. **52:**229–246. http://dx.doi.org/10.1093/jac/dkg321.
9. **Riedel S, Beekmann SE, Heilmann KP, Richter SS, Garcia-de-Lomas J, Ferech M, Goosens H, Doern GV.** 2007. Antimicrobial use in Europe and antimicrobial resistance in *Streptococcus pneumoniae*. Eur. J. Clin. Microbiol. Infect. Dis. **26:**485–490. http://dx.doi.org/10.1007/s10096-007-0321-5.
10. **de la Campa AG, Ardanuy C, Balsalobre L, Pérez-Trallero E, Marimón JM, Fenoll A, Liñares J.** 2009. Changes in fluoroquinolone-resistant *Streptococcus pneumoniae* after 7-valent conjugate vaccination, Spain. Emerg. Infect. Dis. **15:**905–911. http://dx.doi.org/10.3201/eid1506.080684.
11. **Fuller JD, McGeer A, Low DE.** 2005. Drug-resistant pneumococcal pneumonia: clinical relevance and approach to management. Eur. J. Clin. Microbiol. Infect. Dis. **24:**780–788. http://dx.doi.org/10.1007/s10096-005-0059-x.
12. **Adam HJ, Hoban DJ, Gin AS, Zhanel GG.** 2009. Association between fluoroquinolone usage and a dramatic rise in ciprofloxacin-resistant *Streptococcus pneumoniae* in Canada, 1997–2006. Int. J. Antimicrob. Agents **34:**82–85. http://dx.doi.org/10.1016/j.ijantimicag.2009.02.002.
13. **Chen DK, McGeer A, de Azavedo JC, Low DE.** 1999. Decreased susceptibility of Streptococcus pneumoniae to fluoroquinolones in Canada. N. Engl. J. Med. **341:**233–239. http://dx.doi.org/10.1056/NEJM199907223410403.
14. **Drlica K, Zhao X.** 1997. DNA gyrase, topoisomerase IV, and the 4-quinolones. Microbiol. Mol. Biol. Rev. **61:**377–392.
15. **Muñoz R, de La Campa AG.** 1996. ParC subunit of DNA topoisomerase IV of Streptococcus pneumoniae is a primary target of fluoroquinolones and cooperates with DNA gyrase A subunit in forming resistance phenotype. Antimicrob. Agents Chemother. **40:**2252–2257.
16. **Janoir C, Zeller V, Kitzis M-D, Moreau NJ, Gutmann L.** 1996. High-level fluoroquinolone resistance in *Streptococcus pneumoniae* requires mutations in *parC* and *gyrA*. Antimicrob. Agents Chemother. **40:**2760–2764.
17. **Fernández-Moreira E, Balas D, González I, de la Campa AG.** 2000. Fluoroquinolones inhibit preferentially *Streptococcus pneumoniae* DNA topoisomerase IV than DNA gyrase native proteins. Microb. Drug Resist. **6:**259–267. http://dx.doi.org/10.1089/mdr.2000.6.259.

18. **Tankovic J, Perichon B, Duval J, Courvalin P.** 1996. Contribution of mutations in *gyrA* and *parC* genes to fluoroquinolone resistance of mutants of *Streptococcus pneumoniae* obtained in vivo and in vitro. Antimicrob. Agents Chemother. **40:**2505–2510.

19. **Houssaye S, Gutmann L, Varon E.** 2002. Topoisomerase mutations associated with in vitro selection of resistance to moxifloxacin in *Streptococcus pneumoniae*. Antimicrob. Agents Chemother. **46:**2712–2715. http://dx.doi.org/10.1128/AAC.46.8.2712-2715.2002.

20. **Champoux JJ.** 2001. DNA topoisomerases: structure, function, and mechanism. Annu. Rev. Biochem. **70:**369–413. http://dx.doi.org/10.1146/annurev.biochem.70.1.369.

21. **Gellert M, Mizuuchi K, ODea H, Nash HA.** 1976. DNA gyrase: an enzyme that introduces superhelical turns into DNA. Proc. Natl. Acad. Sci. U. S. A. **73:**3872–3876. http://dx.doi.org/10.1073/pnas.73.11.3872.

22. **Kato J, Nishimura Y, Imamura R, Niki H, Hiraga S, Suzuki H.** 1990. New topoisomerase essential for chromosome segregation in *E. coli*. Cell **63:**393–404. http://dx.doi.org/10.1016/0092-8674(90)90172-B.

23. **Tse-Dinh Y-C.** 1985. Regulation of the *Escherichia coli* DNA topoisomerase I gene by DNA supercoiling. Nucleic Acids Res. **13:**4751–4763. http://dx.doi.org/10.1093/nar/13.13.4751.

24. **Menzel R, Gellert M.** 1983. Regulation of the genes for *E. coli* DNA gyrase: homeostatic control of DNA supercoiling. Cell **34:**105–113. http://dx.doi.org/10.1016/0092-8674(83)90140-X.

25. **Menzel R, Gellert M.** 1987. Modulation of transcription by DNA supercoiling: a deletion analysis of the *Escherichia coli gyrA* and *gyrB* promoters. Proc. Natl. Acad. Sci. U. S. A. **84:**4185–4189. http://dx.doi.org/10.1073/pnas.84.12.4185.

26. **Menzel R, Gellert M.** 1987. Fusions of the *Escherichia coli gyrA* and *gyrB* control regions to the galactokinase gene are inducible by coumermycin treatment. J. Bacteriol. **169:**1272–1278.

27. **Peter BJ, Arsuaga J, Breier AM, Khodursky AB, Brown PO, Cozzarelli NR.** 2004. Genomic transcriptional response to loss of chromosomal supercoiling in *Escherichia coli*. Genome Biol. **5:**R87. http://dx.doi.org/10.1186/gb-2004-5-11-r87.

28. **Jeong KS, Xie Y, Hiasa H, Khodursky AB.** 2006. Analysis of pleiotropic transcriptional profiles: a case study of DNA gyrase inhibition. PLoS Genet. **2:**e152. http://dx.doi.org/10.1371/journal.pgen.0020152.

29. **Gmüender H, Kuratli KK, Di Padova CP, Gray W, Keck W, Evers S.** 2001. Gene expression changes triggered by exposure of *Haemophilus influenzae* to novobiocin or ciprofloxacin: combined transcription and translation analysis. Genome Res. **11:**28–42. http://dx.doi.org/10.1101/gr.157701.

30. **Ferrándiz MJ, Martín-Galiano AJ, Schvartzman JB, de la Campa AG.** 2010. The genome of *Streptococcus pneumoniae* is organized in topology-reacting gene clusters. Nucleic Acids Res. **38:**3570–3581. http://dx.doi.org/10.1093/nar/gkq106.

31. **Drlica K, Malik M, Kerns RJ, Zhao X.** 2008. Quinolone-mediated bacterial death. Antimicrob. Agents Chemother. **52:**385–392. http://dx.doi.org/10.1128/AAC.01617-06.

32. **Wang X, Zhao X, Malik M, Drlica K.** 2010. Contribution of reactive oxygen species to pathways of quinolone-mediated bacterial cell death. J. Antimicrob. Chemother. **65:**520–524. http://dx.doi.org/10.1093/jac/dkp486.

33. **Imlay JA, Chin SM, Linn S.** 1988. Toxic DNA damage by hydrogen peroxide through the Fenton reaction in vivo and in vitro. Science **240:**640–642. http://dx.doi.org/10.1126/science.2834821.

34. **Dwyer DJ, Kohanski MA, Hayete B, Collins JJ.** 2007. Gyrase inhibitors induce an oxidative damage cellular death pathway in *Escherichia coli*. Mol. Syst. Biol. **3:**91. http://dx.doi.org/10.1038/msb4100135.

35. **Kohanski MA, Dwyer DJ, Hayete B, Lawrence CA, Collins JJ.** 2007. A common mechanism of cellular death induced by bactericidal antibiotics. Cell **130:**797–810. http://dx.doi.org/10.1016/j.cell.2007.06.049.

36. **Wang X, Zhao X.** 2009. Contribution of oxidative damage to antimicrobial lethality. Antimicrob. Agents Chemother. **53:**1395–1402. http://dx.doi.org/10.1128/AAC.01087-08.

37. **Yeom J, Imlay JA, Park W.** 2010. Iron homeostasis affects antibiotic-mediated cell death in *Pseudomonas* species. J. Biol. Chem. **285:**22689–22695. http://dx.doi.org/10.1074/jbc.M110.127456.

38. **Imlay JA.** 2013. The molecular mechanisms and physiological consequences of oxidative stress: lessons from a model bacterium. Nat. Rev. Microbiol. **11:**443–454. http://dx.doi.org/10.1038/nrmicro3032.

39. **Foti JJ, Devadoss B, Winkler JA, Collins JJ, Walker GC.** 2012. Oxidation of the guanine nucleotide pool underlies cell death by bactericidal antibiotics. Science **336:**315–319. http://dx.doi.org/10.1126/science.1219192.

40. **Liu Y, Imlay JA.** 2013. Cell death from antibiotics without the involvement of reactive oxygen species. Science **339:**1210–1213. http://dx.doi.org/10.1126/science.1232751.

41. **Keren I, Wu Y, Inocencio J, Mulcahy LR, Lewis K.** 2013. Killing by bactericidal antibiotics does not depend on reactive oxygen species. Science **339:**1213–1216. http://dx.doi.org/10.1126/science.1232688.

42. **Dorsey-Oresto A, Lu T, Mosel M, Wang X, Salz T, Drlica K, Zhao X.** 2013. YihE kinase is a central regulator of programmed cell death in bacteria. Cell Rep. **3:**528–537. http://dx.doi.org/10.1016/j.celrep.2013.01.026.

43. **Kohanski MA, Dwyer DJ, Wierzbowski J, Cottarel G, Collins JJ.** 2008. Mistranslation of membrane proteins and two-component system activation trigger antibiotic-mediated cell death. Cell **135:**679–690. http://dx.doi.org/10.1016/j.cell.2008.09.038.

44. **Lacks SA, López P, Greenberg B, Espinosa M.** 1986. Identification and analysis of genes for tetracycline resistance and replication functions in the broad-host-range plasmid pLS1. J. Mol. Biol. **192:**753–765. http://dx.doi.org/10.1016/0022-2836(86)90026-4.

45. **Balsalobre L, de la Campa AG.** 2008. Fitness of *Streptococcus pneumoniae* fluoroquinolone-resistant strains with topoisomerase IV recombinant genes. Antimicrob. Agents Chemother. **52:**822–830. http://dx.doi.org/10.1128/AAC.00731-07.

46. **Fani F, Leprohon P, Legare D, Ouellette M.** 2011. Whole genome sequencing of penicillin-resistant *Streptococcus pneumoniae* reveals mutations in penicillin-binding proteins and in a putative iron permease. Genome Biol. **12:**R115. http://dx.doi.org/10.1186/gb-2011-12-11-r115.

47. **Pruss GJ, Manes SH, Drlica K.** 1982. *Escherichia coli* DNA topoisomerase I mutants: increased supercoiling is corrected by mutations near gyrase genes. Cell **31:**35–42. http://dx.doi.org/10.1016/0092-8674(82)90402-0.

48. **Claverys JP, Prudhomme M, Martin B.** 2006. Induction of competence regulons as a general response to stress in gram-positive bacteria. Annu. Rev. Microbiol. **60:**451–475. http://dx.doi.org/10.1146/annurev.micro.60.080805.142139.

49. **Luo P, Morrison DA.** 2003. Transient association of an alternative sigma factor, ComX, with RNA polymerase during the period of competence for genetic transformation in *Streptococcus pneumoniae*. J. Bacteriol. **185:**349–358. http://dx.doi.org/10.1128/JB.185.1.349-358.2003.

50. **Peterson SN, Sung CK, Cline R, Desai BV, Snesrud EC, Luo P, Walling J, Li H, Mintz M, Tsegaye G, Burr PC, Do Y, Ahn S, Gilbert J, Fleischmann RD, Morrison DA.** 2004. Identification of competence pheromone responsive genes in *Streptococcus pneumoniae* by use of DNA microarrays. Mol. Microbiol. **51:**1051–1070. http://dx.doi.org/10.1046/j.1365-2958.2003.03907.x.

51. **Dagkessamanskaia A, Moscoso M, Henard V, Guiral S, Overweg K, Reuter M, Martin B, Wells J, Claverys JP.** 2004. Interconnection of competence, stress and CiaR regulons in *Streptococcus pneumoniae*: competence triggers stationary phase autolysis of ciaR mutant cells. Mol. Microbiol. **51:**1071–1086. http://dx.doi.org/10.1111/j.1365-2958.2003.03892.x.

52. **Ween O, Gaustad P, Havarstein LS.** 1999. Identification of DNA binding sites for ComE, a key regulator of natural competence in *Streptococcus pneumoniae*. Mol. Microbiol. **33:**817–827. http://dx.doi.org/10.1046/j.1365-2958.1999.01528.x.

53. **Lee MS, Morrison DA.** 1999. Identification of a new regulator in *Streptococcus pneumoniae* linking quorum sensing to competence for genetic transformation. J. Bacteriol. **181:**5004–5016.

54. **de Saizieu A, Gardes C, Flint N, Wagner C, Kamber M, Mitchell TJ, Keck W, Amrein KE, Lange R.** 2000. Microarray-based identification of a novel *Streptococcus pneumoniae* regulon controlled by an autoinduced peptide. J. Bacteriol. **182:**4696–4703. http://dx.doi.org/10.1128/JB.182.17.4696-4703.2000.

55. **Reichmann P, Hakenbeck R.** 2000. Allelic variation in a peptide-inducible two-component system of *Streptococcus pneumoniae*. FEMS Microbiol. Lett. **190:**231–236. http://dx.doi.org/10.1111/j.1574-6968.2000.tb09291.x.

56. **Ulijasz AT, Andes DR, Glasner JD, Weisblum B.** 2004. Regulation of iron transport in *Streptococcus pneumoniae* by RitR, an orphan response regulator. J. Bacteriol. **186:**8123–8136. http://dx.doi.org/10.1128/JB.186.23.8123-8136.2004.

57. **Muñoz R, Bustamante M, de la Campa AG.** 1995. Ser-127-to-Leu substitution in the DNA gyrase B subunit of *Streptococcus pneumoniae* is implicated in novobiocin resistance. J. Bacteriol. **177:**4166–4170.

58. **García MT, Blázquez MA, Ferrándiz MJ, Sanz MJ, Silva-Martín N, Hermoso JA, de la Campa AG.** 2011. New alkaloid antibiotics that target

the DNA topoisomerase I of *Streptococcus pneumoniae*. J. Biol. Chem. **286:**6402–6413. http://dx.doi.org/10.1074/jbc.M110.148148.

59. **Spellerberg B, Cundell DR, Sandros J, Pearce BJ, Idanpaan-Heikkila I, Rosenow C, Masure HR.** 1996. Pyruvate oxidase, as a determinant of virulence in *Streptococcus pneumoniae*. Mol. Microbiol. **19:**803–813.

60. **Prudhomme M, Attaiech L, Sanchez G, Martin B, Claverys JP.** 2006. Antibiotic stress induces genetic transformability in the human pathogen *Streptococcus pneumoniae*. Science **313:**89–92. http://dx.doi.org/10.1126/science.1127912.

61. **Snyder M, Drlica K.** 1979. DNA gyrase on the bacterial chromosome: DNA cleavage induced by oxolonic acid. J. Mol. Biol. **131:**287–302.

62. **Rosch JW, Gao G, Ridout G, Wang YD, Tuomanen EI.** 2009. Role of the manganese efflux system mntE for signalling and pathogenesis in *Streptococcus pneumoniae*. Mol. Microbiol. **72:**12–25. http://dx.doi.org/10.1111/j.1365-2958.2009.06638.x.

63. **Martín-Galiano AJ, Overweg K, Ferrándiz MJ, Reuter M, Wells JM, de la Campa AG.** 2005. Transcriptional analysis of the acid tolerance response in *Streptococcus pneumoniae*. Microbiology **151:**3935–3946. http://dx.doi.org/10.1099/mic.0.28238-0.

64. **Bortoni ME, Terra VS, Hinds J, Andrew PW, Yesilkaya H.** 2009. The pneumococcal response to oxidative stress includes a role for Rgg. Microbiology **155:**4123–4134. http://dx.doi.org/10.1099/mic.0.028282-0.

65. **Hendriksen WT, Bootsma HJ, Estevao S, Hoogenboezem T, de Jong A, de Groot R, Kuipers OP, Hermans PW.** 2008. CodY of *Streptococcus pneumoniae*: link between nutritional gene regulation and colonization. J. Bacteriol. **190:**590–601. http://dx.doi.org/10.1128/JB.00917-07.

66. **Caymaris S, Bootsma HJ, Martin B, Hermans PW, Prudhomme M, Claverys JP.** 2010. The global nutritional regulator CodY is an essential protein in the human pathogen *Streptococcus pneumoniae*. Mol. Microbiol. **78:**344–360. http://dx.doi.org/10.1111/j.1365-2958.2010.07339.x.

67. **Manzor ISS, Klosterman TG, Kuipers OP.** 2013. Transcriptional response of *Streptococcus pneumoniae* to varying sources of iron and the regulatory mechanism of iron uptake system PiuBCDA, abstr OGE02. XI Eur. Meet. Mol. Biol. Pneumococcus (EuroPneumo 2013), Madrid, Spain.

68. **Martín-Galiano AJ, Ferrándiz MJ, de la Campa AG.** 2001. The promoter of the operon encoding the F_0F_1 ATPase of *Streptococcus pneumoniae* is inducible by pH. Mol. Microbiol. **41:**1327–1338. http://dx.doi.org/10.1046/j.1365-2958.2001.02597.x.

69. **Frawley ER, Crouch ML, Bingham-Ramos LK, Robbins HF, Wang W, Wright GD, Fang FC.** 2013. Iron and citrate export by a major facilitator superfamily pump regulates metabolism and stress resistance in *Salmonella typhimurium*. Proc. Natl. Acad. Sci. U. S. A. **110:**12054–12059. http://dx.doi.org/10.1073/pnas.1218274110.

70. **Pericone CD, Overweg K, Hermans PWM, Weiser JN.** 2000. Inhibitory and bactericidal effects of hydrogen peroxide production by *Streptococcus pneumoniae* on other inhabitants of the upper respiratory tract. Infect. Immun. **68:**3990–3997. http://dx.doi.org/10.1128/IAI.68.7.3990-3997.2000.